applied sciences

MDPI

Article

Comparison of Grinding Characteristics of Converter Steel Slag with and without Pretreatment and Grinding Aids

Jihui Zhao [1,*], Dongmin Wang [2], Peiyu Yan [1] and Wenping Li [2]

[1] Institute of Building Materials, Department of Civil Engineering, Tsinghua University, Beijing 100084, China; yanpy@tsinghua.edu.cn

[2] School of Chemical & Environmental Engineering, China University of Mining & Technology, Beijing 100083, China; wangdongmin-2008@163.com (D.W.); lwpchina@163.com (W.L.)

* Correspondence: zhaojihui324@163.com; Tel.: +86-159-0124-5174

Academic Editor: Stefano Invernizzi

Received: 10 June 2016; Accepted: 8 August 2016; Published: 28 October 2016

Abstract: The converter steel slag cannot be widely used in building materials for its poor grindability. In this paper, the grinding characteristics of untreated and pretreated (i.e., magnetic separation) steel slag were compared. Additionally, the grinding property of pretreated steel slag was also studied after adding grinding aids. The results show that the residues (i.e., oversize substance) that passed a 0.9 mm square-hole screen can be considered as the hardly grinding phases (HGP) and its proportion is about 1.5%. After the initial 20 min grinding, the RO phase (RO phase is a continuous solid solution which is composed of some divalent metal oxides, such as FeO, MgO, MnO, CaO, etc.), calcium ferrite, and metallic iron phase made up most of the proportion of the HGP, while the metallic iron made up the most component after 70 min grinding. The D50 of untreated steel slag could only reach 32.89 μm after 50 min grinding, but that of pretreated steel slag could reach 18.16 μm after the same grinding time. The grinding efficiency of steel slag was obviously increased and the particle characteristics were improved after using grinding aids (GA), especially the particle proportions of 3–32 μm were obviously increased by 7.24%, 7.22%, and 10.63% after 40 min, 50 min, and 60 min grinding, respectively. This is mainly because of the reduction of agglomeration and this effect of GA was evidenced by SEM (scanning electron microscope) images.

Keywords: steel slag; grinding property; particle characteristics; mineral phase; hardly grinding phases; magnetic separation; grinding aids; agglomeration

1. Introduction

Steel slag is an industrial solid waste generated in the steel-making process, but it is rich in dicalcium silicate (C_2S) and tricalcium silicate (C_3S) in mineral compositions, which is similar to cement clinker [1–4]. Based on its mineral compositions, steel slag has great potential for application as supplementary cementitious materials (also known as mineral admixture) of cement and concrete [5–8]. Generally, only after being ground into powder, could steel slag have hydration activity and be used as supplementary cementitious materials [9,10]. The smaller the particle size of steel slag powder, the higher its hydration activity [11,12]. However, the grindability of steel slag is much worse than that of other mineral admixtures such as fly ash and granulated blast-furnace slag, seriously impeding the preparation efficiency of steel slag powder and its application performance in building materials. Therefore, its grinding property is an important consideration in the application of steel slag.

In the grinding process of a solid, particles characteristics such as size, distribution, bulk density, and dispersion are in constant change on a macroscopic scale, and the internal chemical bonds of

particles are constantly broken on a microscopic scale [13–15]. Steel slag has poor grindability because of a large amount of iron oxides and continuous solid solution composed of some divalent metal oxides, which form a dense structure in the steel slag [16,17]. Currently, the researches on improvement of grinding efficiency for steel slag mainly focus on the optimization of grinding equipment—such as vertical mill and roller mill, while there are few researches on other measures, such as removal of hardly grinding phases (HGP) or the use of chemical admixtures. Although vertical mills have been applied in grinding of steel slag, many application researches indicate that steel slag powder prepared by vertical mills have poor particle morphology—such as flat, needle, and irregular shapes, resulting in the ball mill still being chosen by many manufacturers to prepare steel slag powder in China. Meanwhile, some studies indicate that metallic iron in steel slag is one main reason causing its poor grinding property. However, in different grinding periods, the factors influencing grinding efficiency usually change due to different grinding characteristics [18–20], but to date these factors have not been yet been fully studied. Some researches also show that the split-phase phenomenon occurs in the grinding process of steel slag, resulting in ground steel slag powder having some differences in chemical and mineral compositions during different grinding periods [21,22]. So, it is necessary to reveal the factors influencing the grinding efficiency of steel slag from studying grinding characteristics, hardly grinding phases, and split-phase phenomenon during different grinding periods. Moreover, in the grinding process of a solid, other phenomena such as agglomeration of fine particles and re-healing of particle fracture surfaces result in a lower grinding efficiency and higher energy consumption [23–26]. In recent years, grinding aids, most of which are polar organic compounds, are extensively applied to weaken agglomeration of fine particles and improve grinding efficiency of cement [27]. Therefore, the use of grinding aids is also an important way to improve preparation efficiency of steel slag powder.

Based on the abovementioned discussion, the hardly grinding phases of converter steel slag were revealed from the proportion, morphology, mineral, and chemical compositions. Then the grinding characteristics of untreated and pretreated (i.e., magnetic separation) steel slag were compared from the proportion of iron phases, grinding efficiency, particle size, and particle distribution and morphology. Further, the grinding property of pretreated steel slag was also studied after adding organic grinding aids and its positive role and mechanism were discussed here as well.

2. Materials and Methods

2.1. Materials

The converter steel slag used was provided from Laiwu Steel Corporation (Laiwu, China). The chemical compositions of steel slag, which were determined by X-ray fluorescence (XRF) analysis, (Rh, 40 kV, 70 mA), are given in Table 1. The mineral phases of steel slag, which were analyzed by X-ray diffraction (XRD), using a D6000 diffractometer with nickel-filtered Cu Kαl radiation (= 1.5405 Å, 40 kV, and 40 mA) from Shimadzu company (Kyoto, Japan), are given in Figure 1. The organic grinding aid used, produced by Sinopharm Chemical Reagent Beijing Co., Ltd. (Beijing, China), was chemical grade glycerol.

Table 1. Chemical compositions of converter steel slag (%).

CaO	SiO_2	Al_2O_3	Fe_2O_3	MgO	K_2O	SO_3	P_2O_5	LOI
39.67	21.71	1.58	25.52	4.92	0.02	0.18	1.70	0.32

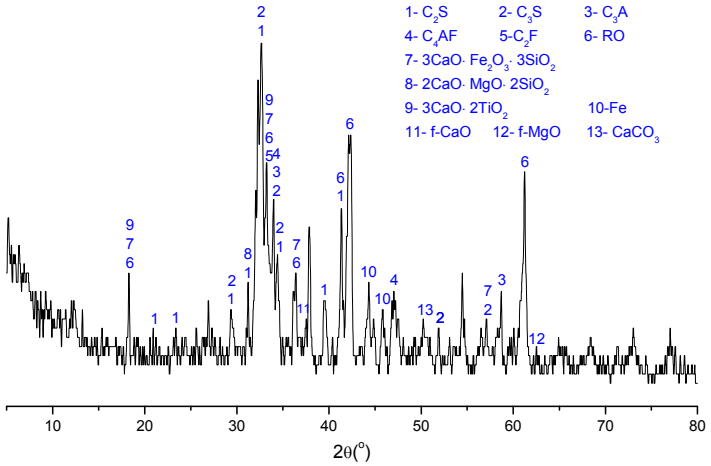

Figure 1. X-ray diffraction (XRD) pattern of converter steel slag.

2.2. Experimental Methods

2.2.1. Observation and Identification of Mineral Phases for Converter Steel Slag

The steel slag sample needed to be prepared for the morphology observation of mineral phase. Firstly, the surface of the 3–8 mm blocky steel slag was burnished using P200#, P400#, P600#, P800#, P1000#, and P1200# sandpapers in turn, and was then polished by a polisher (UNIPOL-830, Shenyang Kejing Instrument Co., Ltd., Shenyang, China). The mineral phases were observed and identified by back-scattered electron (BSE) imaging and energy dispersive X-ray spectroscopy (EDX), respectively, using a scanning electron microscope (Quanta 200 FEG, FEI Company, Hillsboro, OR, USA). In addition, the hardly grinding phases were observed using a metallographic microscope (BA210Met, Motic China Group Co., Ltd., Xiamen, China).

2.2.2. Measurement of Vickers Hardness of Mineral Phases for Converter Steel Slag

The Vickers hardness of different mineral phases for steel slag was measured using a Vickers hardness tester (HV-1000, Shanghai Materials Tester Factory, Shanghai, China), and the hardness value of each mineral phase was determined by taking the average of multiple points.

2.2.3. Procedure of Grinding Experiment for Steel Slag

Grinding experiments of steel slag were carried out by laboratory ball mill (SM-500, Wuxi Jianyi Experiment Instrument Co., Ltd., Wuxi, China). The type of the ball mill was Φ500 mm × 500 mm, 48 r/min, and the grinding media was composed of 60 kg steel balls (Φ40 mm, Φ50 mm, Φ60 mm, and Φ70 mm) and 40 kg small steel forgings (Φ25 mm × 35 mm).

The steel slag was firstly crushed to less than 5 mm by a jaw crusher (PE 60 × 100, Shanghai Longshi Machinery Co., Ltd., Shanghai, China) before the grinding experiment. The weight of steel slag for each grinding experiment was 3 kg and the grinding times were 10 min, 20 min, 30 min, 40 min, 50 min, 60 min, and 70 min. In addition, for the grinding aids experiment, 0.05% grinding aid was added into the test group to compare with the blank group (i.e., without any grinding aids).

2.2.4. Test Methods of Particle Size and Distribution of Ground Steel Slag Powder

The specific surface area of ground steel slag powder was measured by Blaine method, conforming to Chinese National Standard GB/T8074-2008. The sieving residue of steel slag powder was measured by sieving analysis method with a 45 μm square-hole screen, conforming to the Chinese National Standard GB/T1345-2005. The particle size distribution was measured by laser-scattering method, conforming to the Chinese Industry Standard JC/T721-2006.

2.2.5. Observation of Particle Morphology of Ground Steel Slag Powder

The particle morphology of ground steel slag powder was observed with a scanning electron microscope (Quanta 200 FEG, FEI Company, Hillsboro, OR, USA) under high vacuum condition.

2.2.6. Test Methods of the Angle of Repose of Ground Steel Slag Powder

The angle of repose of ground steel slag powder was tested conforming to the Chinese National Standard GB/T11986-1989, as follows: steel slag powder was poured into a funnel, and then powder from the funnel fell onto and coated the disc below the funnel. Then the height, h, of the powder layer and the radius, R, of the disc were measured, thus the angle of repose, θ, of steel slag powder was obtained according to the formula ($\tan\theta = h/R$).

3. Results and Discussion

3.1. Mineral Phases'Characteristics of Converter Steel Slag

As shown in Figure 2a, the morphologies of mineral phases in steel slag show different grey levels under BSE images, such as black, grey-black, grey, light-grey, and white-bright in grey level, which exhibit different shapes as well, such as round shape, leaf-like shape, hexagonal-plate shape, irregular shape, and so on. The compositions of these minerals with different grey levels were determined using EDX analysis, and the results are shown in Figure 2b. It can be seen from EDX analysis results that the minerals with grey levels of black and grey-black are mainly the silicate minerals phases which are composed of oxygen, silicon, and calcium elements; the irregular mineral phases with grey level of light-grey are mainly RO phase which is composed of oxygen, magnesium, calcium, manganese, and iron elements; the irregular-shaped minerals with grey level of grey, which are filled in light-grey and black minerals, are the calcium ferrite phases mainly composed of oxygen, calcium, iron, aluminum, and silicon elements; the round granular-shaped minerals with grey level of white-bright are the metallic iron phase. The above results show that the mineral phases of steel slag mainly contain silicate mineral phase, RO phase, calcium ferrite phase, and a small amount of metallic iron phase, etc. It is also evident from XRD analysis presented in Figure 1 that the mineral phases converter steel slag mainly contains C_2S, C_3S, RO, $3CaO{\cdot}Fe_2O_3{\cdot}3SiO_2$ (i.e., calcium ferrite phases) and so on. (Comment: RO phase is a continuous solid solution which is composed of some divalent metal oxides, such as FeO, MgO, MnO, CaO, etc.)

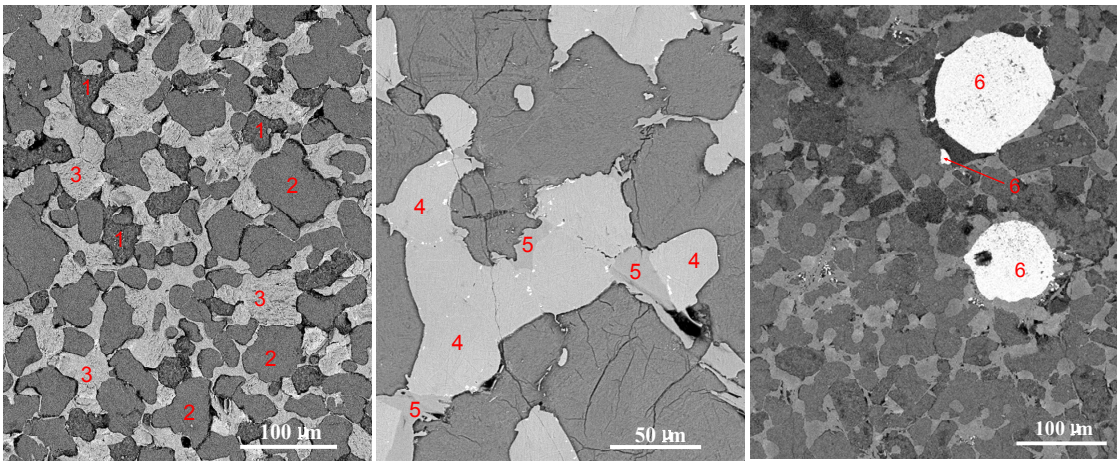

(**a**)

Figure 2. *Cont.*

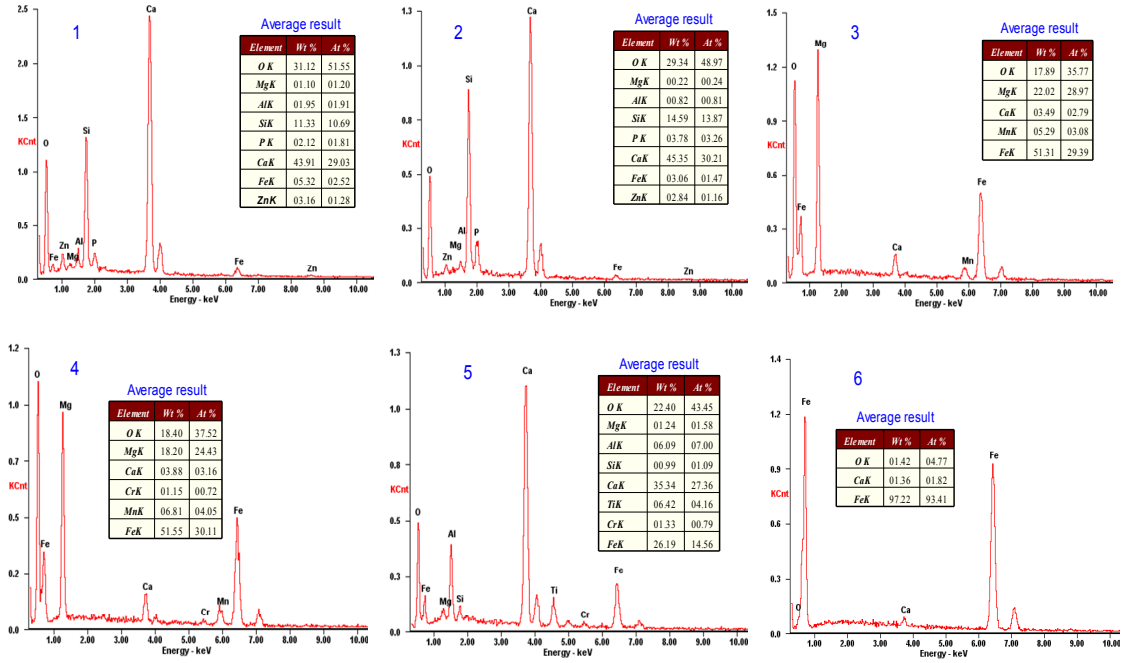

(**b**)

Figure 2. Morphologies and identification of mineral phases in converter steel slag. (**a**): Back-scattered electron (BSE) images of various mineral phases; (**b**) Energy dispersive X-ray spectroscopy (EDX) analysis results of various mineral phases.

3.2. Determination of Hardly Grinding Phases (HGP) in Converter Steel Slag

As the grindability of various mineral phases in steel slag have great differences, the easily grinding phases (denoted as EGP) are firstly being ground to fine powder, while the poor grindability mineral phases are difficult to grind down, which seriously affects the grinding efficiency. However, different mineral phases in steel slag are very difficult to be separated out, so it is impossible to determine what is an easily grinding phase and hardly grinding phase from the grindability index of various mineral phases. In this paper, a simple method for determination of the hardly grinding phase in steel slag by oversize substance (i.e., residue) is provided. After grinding and then screening of steel slag powder, the oversize substance obtained can be considered as the hardly grinding phases (denoted as HGP) in steel slag. In order to determine the HGP in the grinding process, the steel slag powder after 10, 20, 30, 40, 50, 60, and 70 min grinding were screened with a 0.9 mm square-hole screen, and then the proportion, morphology, and compositions of oversized substances (i.e., HGP) were analyzed.

3.2.1. Proportion of HGP in Converter Steel Slag

The proportions of oversized substances after different grinding times are shown in Figure 3. Form the figure, with the increasing of grinding time of steel slag, the proportion of oversized substances that passed the 0.9 mm square-hole screen rapidly declined in the range of 10–20 min grinding time, and then starts to slowly decline (starting from 30 min grinding time), until the proportion finally reaches about 1.5%, which indicates that this part of oversize substances is the HGP in converter steel slag. In other words, the proportion of HGP determined by residue method of 0.9 mm square-hole screen is about 1.5%.

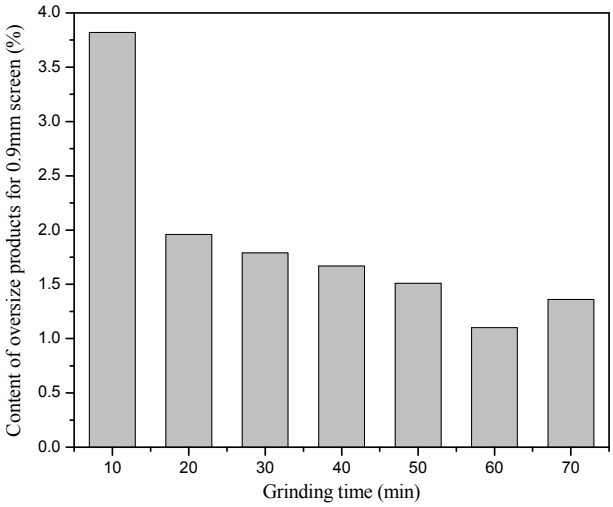

Figure 3. Proportion of oversize substances of steel slag powder vs. grinding time.

3.2.2. Morphology and Vickers Hardness of HGP in Converter Steel Slag

As shown in Figure 4, the morphology of HGP in converter steel slag mainly shows three kinds of grey levels during the initial grinding period (20 min grinding time), while basically exhibiting one grey level during the middle–later grinding periods (i.e., 50 min and 70 min grinding times). Based on the identification and analysis results of mineral phases in Section 3.1, it can be known that the mineral phases with three kinds of grey levels are mainly the RO phase, calcium ferrite, and metallic iron phase. So, the HGP of converter steel slag during the initial grinding period is composed of RO phase, calcium ferrite, and metallic iron phase, while the HGP is mainly the metallic iron phase during the later grinding period, and the longer grinding time, the higher the proportion of metallic iron phase.

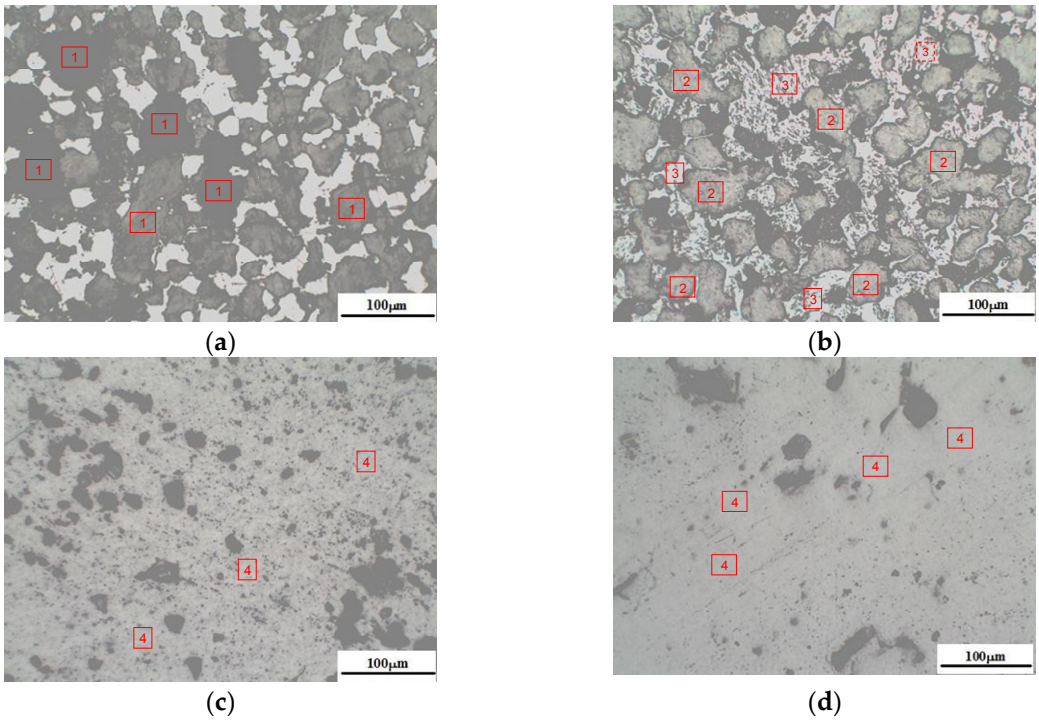

Figure 4. Morphologies of oversize substances of steel slag powder vs. grinding time: (**a**) 0 min; (**b**) 20 min; (**c**) 50 min; (**d**) 70 min.

To reflect HGP characteristics from another point of view, the Vickers hardness of selected regions in Figure 4 were tested and results are shown in Table 2. To some extent, the hardness of the mineral phase can reflect its grindability. Results of Vicker hardness show that the RO phase and calcium ferrite phase have high hardness compared with the silicate phase, which may be one reason why these two mineral phases are HGP. Meanwhile, metallic iron phase with very low hardness is also HGP because of its high flexibility. Thus, the HGP is explained from Vickers hardness of mineral phases.

Table 2. Vickers hardness of selected region in Figure 4 (HV).

Region number	1	2	3	4
Mineral phases	Silicate phase	Calcium ferrite phase	RO phase	Metallic iron phase
Vickers hardness	187.3	335.0	298.1	29.4

3.2.3. Chemical Compositions of HGP in Converter Steel Slag

The chemical compositions of oversized substances passed a 0.9 mm square-hole screen under different grinding times, which were determined by X-ray fluorescence analysis (XRF) and chemical titration, are shown in Table 3. The results show that the contents of CaO and SiO_2 in HGP gradually decrease with the increase in grinding time, while the contents of metallic iron show a reverse trend, and the contents of Fe_2O_3 and MgO are firstly increased and then decreased with the increasing of grinding time. In the initial grinding period (10–20 min grinding), the chemical compositions of HGP mainly consist of CaO, SiO_2, Fe_2O_3, and MgO; in the middle grinding period (40–50 min grinding), it mainly consists of Fe_2O_3 and metallic iron; in the later grinding period (60–70 min grinding), metallic iron takes up the most component. So the HGP have different chemical compositions during different grinding period.

Table 3. Chemical compositions of hardly grinding phases (HGP) in steel slag vs. grinding time (%).

Grinding time (min)	CaO	SiO_2	Al_2O_3	Fe_2O_3	Fe	MgO
10	32.45	12.05	1.15	34.80	3.53	8.43
20	26.12	8.26	1.06	37.07	7.60	12.29
30	20.30	5.81	0.92	38.13	13.36	13.07
40	14.70	4.16	0.75	39.08	23.10	10.13
50	6.14	3.05	0.62	32.12	45.53	7.20
60	5.19	2.03	0.51	18.09	65.33	4.12
70	4.04	1.14	0.44	11.25	76.20	3.21

3.3. Comparison of Grinding Characteristic between Untreated and Pre-treated Converter Steel Slag

From the research result presented in the previous section, the iron-rich phases, especially metallic iron, are the main hardly grinding phases, so it is necessary to remove or recycle the iron-rich phases before the grinding process of steel slag. In this study, the grinding characteristics of untreated and pretreated converter steel slag were compared with respect to iron mineral phases, grinding efficiency, particle size distribution, and particle morphology (Comment: the pretreatment of steel slag is the preliminary magnetic separation and multistage screening and magnetic separation, as shown in Figure 5).

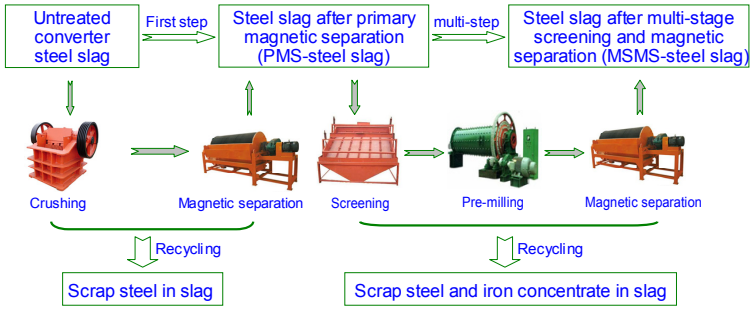

Figure 5. The technical flow process of recycling iron-rich phases in steel slag.

3.3.1. Total Analysis of Iron Mineral Phases in Converter Steel Slag after Pre-treatment

Total analysis results of iron mineral phases in converter steel slag after preliminary magnetic separation (denoted as PMS) and multistage magnetic separation (denoted as SMS) are shown in Table 4.

Table 4. Total analysis results of iron mineral phases in converter steel slag.

Iron mineral phases	Proportions of iron mineral phases (%)		
	Untreated steel slag	PMS-steel slag	SMS-steel slag
Metallic iron & magnetite	2.38	1.18	0.45
Hematite/limonite	13.11	13.05	6.67
Sulfide	0.04	0.04	0.04
Siderite	2.52	2.26	1.98
Iron silicate	0.21	0.10	0.06
Total	18.26	16.63	9.20

From the results, it can be seen that the proportions of iron phases in steel slag are obviously reduced after pretreatment. The proportion of metallic iron in steel slag is decreased from 2.38% to 1.18% by preliminary magnetic separation, and both the metallic iron proportion and total content of iron phases in steel slag are decreased by multistage magnetic separation, from 2.38% to 0.45% and 18.26% to 9.20%, respectively, indicating that the effect of pretreatment on iron-rich phases is obvious. The removal of iron-rich phases in steel slag is a very favorable factor for preparation and application of steel slag powder.

3.3.2. Grinding Efficiency of Untreated and Pretreated Steel Slag

The specific surface areas of untreated and pretreated steel slag under different grinding times are shown in Figure 6.

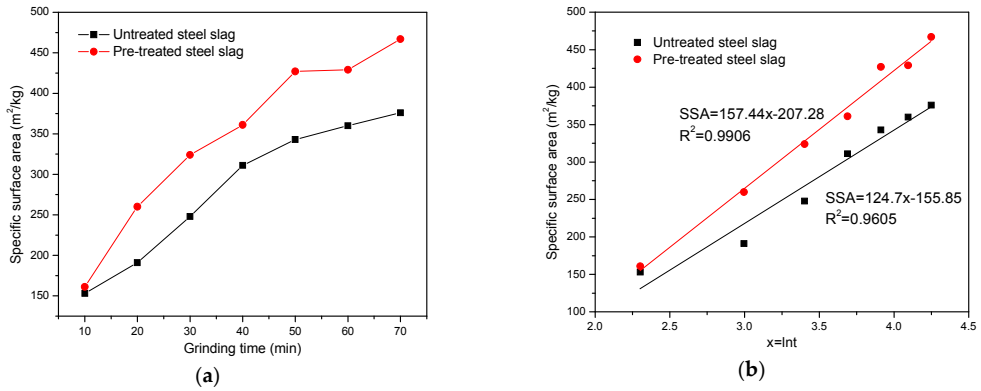

Figure 6. Specific surface areas (SSA) of steel slag under different grinding time: (**a**) SSA vs. grinding time; (**b**) linear fitting of SSA.

As shown in Figure 6, the specific surface areas of untreated and pretreated steel slag are gradually increased with increasing grinding time, and starting from 50 min grinding time, the tendency to increase is slowed down due to the agglomeration of fine particles. The specific surface area of pretreated steel slag is obviously higher than that of untreated steel slag after the same grinding time. For example, the specific surface area of untreated steel slag is only 360 m^2/kg after 60 min grinding, while that of pretreated steel slag reaches 361 m^2/kg after 40 min grinding, thus 20 min grinding time is saved. The relationship of specific surface area vs. grinding time was fitted, and the result is as follows:

$$SSA = 124.7\ln t - 155.85\ (R^2 = 0.9605)\ \text{(Untreated steel slag)} \quad (1)$$

$$SSA = 157.44\ln t - 207.28\ (R^2 = 0.9906)\ \text{(Pretreated steel slag)} \quad (2)$$

From the above fitted result, it can be seen that the relationship of specific surface area with the logarithm of grinding time shows a good linear relationship. After applying derivation calculus to the above equations, we can get the increasing speeds of specific surface area:

$$\frac{dSSA}{dt} = \frac{124.7}{t}\ \text{(Untreated steel slag)} \quad (3)$$

$$\frac{dSSA}{dt} = \frac{157.44}{t}\ \text{(Pretreated steel slag)} \quad (4)$$

It is obvious that the grinding speed of pretreated steel slag is higher than that of untreated steel slag.

3.3.3. Particle Size Distributions of Ground Untreated and Pretreated Steel Slag

The particle size distribution and median diameter of ground untreated and pretreated steel slag powder are shown in Table 5 and Figure 7, respectively.

Table 5. Particle size distribution of ground steel slag powder under different grinding time (%).

Grinding time (min)	Untreated steel slag				Pretreated steel slag			
	<3 μm	3–32 μm	32–65 μm	>65 μm	<3 μm	3–32 μm	32–65 μm	>65 μm
10	2.77	27.88	25.24	44.11	2.44	25.42	21.95	50.19
20	4.97	37.16	27.54	30.33	5.66	40.06	30.84	23.45
30	6.64	36.62	28.04	28.70	9.00	44.22	32.10	14.68
40	8.16	38.24	27.46	26.15	10.54	48.80	30.51	10.15
50	11.18	37.90	22.19	28.73	14.87	56.99	22.65	5.49
60	8.99	32.52	26.57	31.91	16.36	53.83	20.96	8.84
70	10.91	30.99	19.12	38.97	14.50	55.74	21.47	8.29

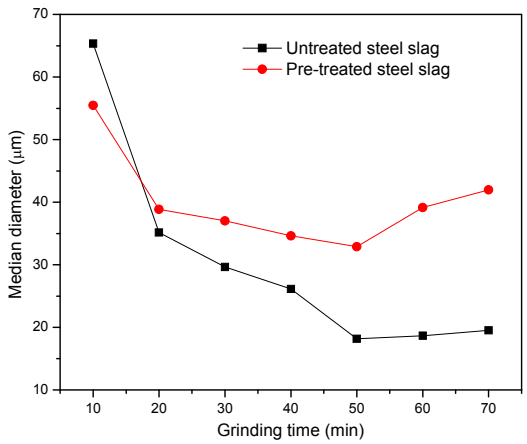

Figure 7. Median diameter of ground steel slag powder under different grinding time.

As shown in Table 5, with increasing grinding time ($\leq$ 50 min), the proportion of particles for more than 32 μm (especially particles for more than 65 μm) is gradually and obviously decreased, while the proportion of particles for less than 32 μm shows a reverse tendency, which indicates that the particle size distribution of steel slag is optimized by mechanical grinding. However, when grinding time is more than 50 min, it shows a complex or chaotic tendency due to the agglomeration of fine particles. Compared with untreated steel slag, the proportion of particles for less than 32 μm in pretreated steel slag powder is much higher after the same grinding time, indicating that the increasing tendency of fine particles for pretreated steel slag powder is faster.

For median diameter (D50), with the increasing of grinding time, the median diameter of steel slag is firstly decreased before 50min grinding time, and then is increased after that, which is similar to the variation tendency of particle proportion of more than 32 μm. At 50 min grinding time, the median diameter of untreated steel slag reaches a minimum, 32.89 μm, which is much larger than that of pretreated steel slag, 18.16 μm. This shows that it is difficult for untreated steel slag to be finely ground.

3.3.4. Particle Morphologies of Ground Untreated and Pretreated Steel Slag

The particle morphologies of two kinds of ground steel slag powder after 50 min grinding are shown in Figure 8. It can be seen from the figure that steel slag particles are mainly spherical in shape, and fine particles adhere to the larger particles. By comparison, the overall particle size of pretreated steel slag powder is smaller than that of untreated steel slag, and particle uniformity in size is also superior to that of untreated steel slag. To some extent, both the ground untreated and pretreated steel slag powders show some agglomeration phenomenon.

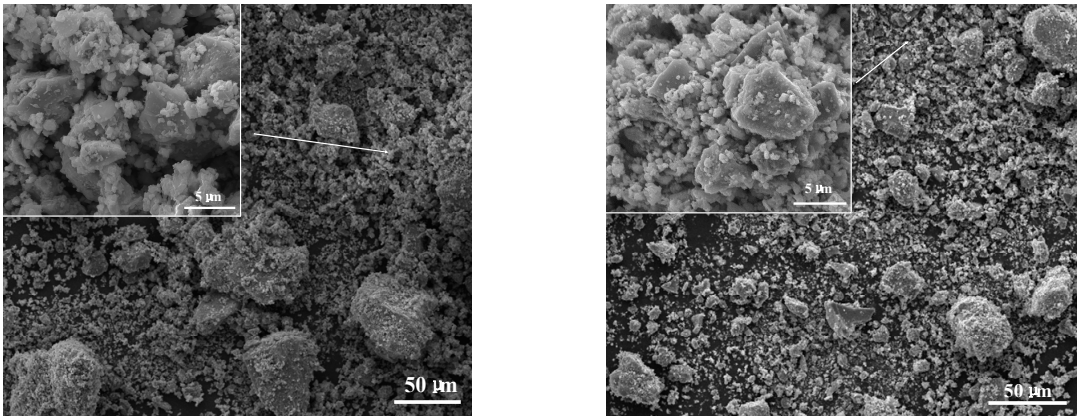

Figure 8. Particle morphology of ground steel slag powder after 50min grinding time: (**a**) untreated steel slag; (**b**) pretreated steel slag.

3.4. Effect of Organic Grinding Aids on the Grinding Property of Converter Steel Slag

From the above results of studies, it can be seen that the agglomeration phenomenon of fine particles will occur during deep grinding periods, which seriously affect or reduce the grinding efficiency of steel slag. In recent years, organic grinding aids (GA) have been used to improve the grinding efficiency of cement. These researches show that organic GA molecules can be adsorbed on the particles and effectively weaken the agglomeration of fine particle in the grinding process, thus improving the dispersion of powder and grinding efficiency [28–31]. Therefore, it is a good choice to use GA in the grinding process of steel slag for many manufacturers to improve preparation efficiency of steel slag powder. In additional, on the basis of pretreatment, the grinding property of steel slag can be further improved by GA. In this study, glycerol, which is a common cement GA, was selected as the GA of steel slag. The effects of GA on the grinding property of steel slag were studied from sieving residue, particle size distribution, angle of repose, and particle morphology.

3.4.1. Effect of GA on the Sieving Residue of Steel Slag Powder

As shown in Figure 9, it can be seen that the sieving residue of steel slag powder with GA is lower than that of the blank group (i.e., without any GA) after the same grinding time, indicating that ground steel slag with GA is smaller in particle size. The reducing effect of GA on the sieving residue is gradually enhanced with the increasing of grinding time before reaching 50 min grinding time. At the initial grinding period (before 20 min), the role of GA is small, but it becomes obvious after 20 min and reaches an optimum grinding role at 50 min grinding time.

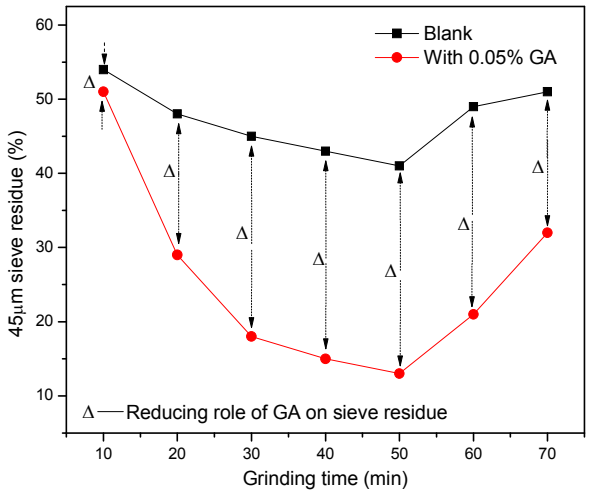

Figure 9. Sieving residue of steel slag powder with grinding aid (GA) vs. grinding time.

3.4.2. Effect of GA on the Particle Size Distribution of Steel Slag Powder

The uniformity coefficient of steel slag powder can reflect the extent of the width of particle size distribution, and the smaller the uniformity coefficient, the wider the particle size distribution. From Figure 10, it can be seen that the uniformity coefficient of steel slag powder is firstly increased and then gradually decreased with the increasing of grinding time. By comparison, the uniformity coefficient of steel slag powder with GA is larger than that without GA for the same grinding time, indicating that the particle size distribution of steel slag powder can be narrowed by GA. The effect is the strongest at 50 min and 60 min grinding times.

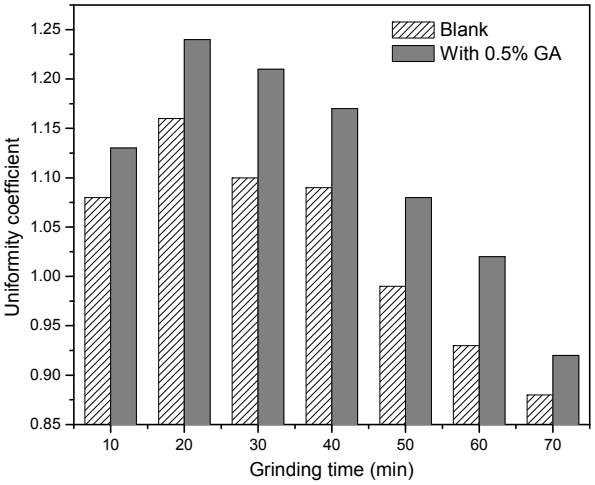

Figure 10. Uniformity coefficient of steel slag powder with GA vs. grinding time.

As shown in Table 6, it can be seen that the effect of GA on the particle size distribution of steel slag powder is relatively small before reaching 40 min grinding time. The reason is that particles are coarse and have a good dispersion at this stage, basically having no agglomeration of fine particles. The grinding efficiency of steel slag is basically not influenced by dispersion of particles, so the optimization role of GA on the particle size distribution is not obvious. During 40 min, 50 min, and 60 min grinding time, the proportions of particles in the range of 3–32 μm are obviously increased by 7.24% (absolute value, same below), 7.22%, and 10.63%, respectively, after adding GA, while the proportions of particles in the range of more than 32 μm are also obviously decreased, indicating that GA can efficiently weaken agglomeration of fine particles, then improve the dispersion of steel slag powder. Meanwhile, many researches indicate that 3–32 μm particles have the greatest contribution on the property of cement-based materials, so the improvement of 3–32 μm particles proportion after using GA shows that GA can significantly optimize particle size distribution of steel slag powder. At 70 min grinding time, as the agglomeration of particles is very serious, GA can not completely resist it due to the fixed dosage (0.05%), resulting in the weakening of GA's optimizing role. It shows that the optimizing role of the fixed dosage GA on the particle size distribution of steel slag powder is different under different grinding times, and the role of 0.05% dosage of GA is best during 40–60 min grinding time.

Table 6. Particle size distribution of steel slag powder with GA under different grinding time (%).

Grinding time (min)	Without GA				With GA			
	<3 μm	3–32 μm	32–65 μm	>65 μm	<3 μm	3–32 μm	32–65 μm	>65 μm
10	2.44	25.42	21.95	50.19	2.83	23.83	22.80	50.54
20	5.66	40.06	30.84	23.45	4.81	37.44	34.14	23.62
30	9.00	44.22	32.10	14.68	7.63	47.08	32.74	12.55
40	10.54	48.80	30.51	10.15	10.44	56.04	28.47	5.04
50	14.87	56.99	22.65	5.49	14.32	64.21	21.10	0.38
60	16.36	53.83	20.96	8.84	15.73	64.46	18.61	1.20
70	14.50	55.74	21.47	8.29	15.05	57.33	19.49	8.13

3.4.3. Effect of GA on the Angle of Repose of Steel Slag Powder

Powder fluidity is usually characterized by the angle of repose. The smaller the angle of repose, the better the powder fluidity. As shown in Figure 11, it can be seen that the angle of repose of steel slag powder is decreased after adding GA, indicating that GA can improve the fluidity of steel slag powder. The role of GA on the angle of repose is firstly enhanced and then weakened on the whole, which is similar to the role of GA on the sieving residue, and it is reaches maximum effectiveness at 50 min grinding time, i.e., the action effect of GA on powder fluidity is the greatest at 50 min grinding time.

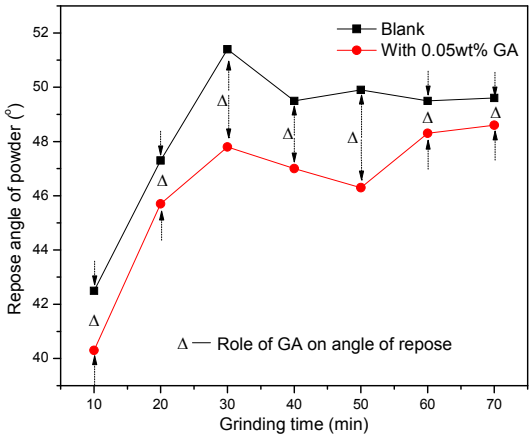

Figure 11. Repose angle of steel slag powder with GA vs. grinding time.

3.4.4. Effect of GA on the Particle Morphology of Steel Slag Powder

The particle morphologies of steel slag powder with and without GA are shown in Figure 12. It can be seen from the figure that the particles of steel slag powder without GA exhibit the agglomeration phenomenon where fine particles adhere to each other. Especially at 70 min grinding time, agglomeration of particles is very serious and many large particles are regenerated by adhering of fine particles. By comparison, after using GA, the agglomeration phenomenon of particles is not obvious at 50min grinding time, still keeping a relatively good dispersion. Although the particles with GA also exhibit a little agglomeration at 70 min grinding time, their dispersion is still obviously better than those without GA. The above results confirm that GA can efficiently weaken the agglomeration of fine particles when particle size becomes small and agglomeration of fine particles occurs.

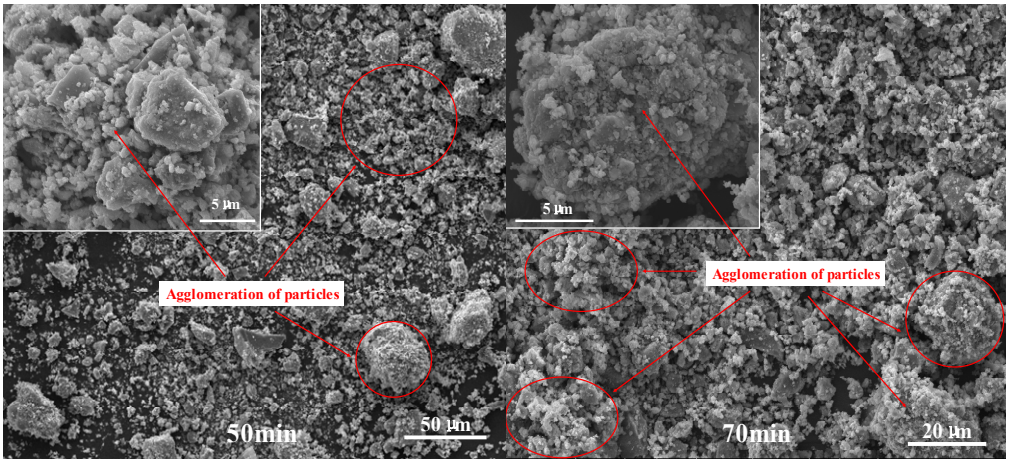

(**a**)

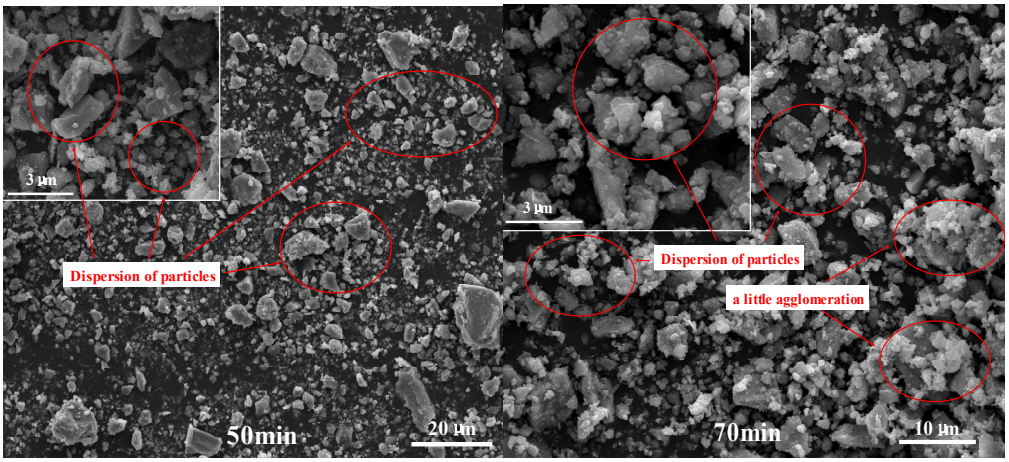

(**b**)

Figure 12. Particle morphologies of steel slag powder with and without GA: (**a**) without GA; (**b**) with GA.

4. Conclusions

From this study, we can conclude that:

(1) It was evident from analysis of BSE–EDX that the mineral phases of converter steel slag mainly contain silicate mineral phase, RO phase, calcium ferrite phase, and a small amount of metallic iron phase, among others.

(2) The oversize substance after screening can be considered as the hardly grinding phases (HGP), which provides a simple method of determining the HGP in steel slag. The HGP proportion which

was determined by a 0.9 mm square-hole screen is about 1.5%. After the initial 20 min grinding, the RO phase, calcium ferrite, and metallic iron phase made up most of the proportion in the HGP, while the metallic iron made up the most component after 70 min grinding.

(3) For steel slag powder with about 360 m^2/kg specific surface area (SSA), 20 min of grinding time can be saved with pretreatment. The relationships of SSA with the logarithm of grinding time show a good linear relationship, but pretreated steel slag has a higher grinding efficiency. In addition, the D50 of untreated steel slag can only reach 32.89 μm after 50 min grinding, but that of pretreated steel slag can reach 18.16 μm after the same grinding time.

(4) Organic grinding aids (GA) can obviously improve the grinding property of steel slag, and the action effects of 0.05% dosage of GA on the grinding efficiency and particle characteristics were the best during 40–60 min grinding time. especially the proportions of particles in the range of 3–32 μm, which were obviously increased by 7.24%, 7.22%, and 10.63% after 40 min, 50 min and 60 min grinding, respectively. This is mainly because of the reduction of agglomeration after the use of GA, as evidenced by SEM images.

Acknowledgments: This work was financially supported by the China's Post-doctoral Science Fund (No. 2016M591170), the Open Fund of Key Laboratory of Advanced Civil Engineering Materials (Tongji University), Ministry of Education (No. 201602).

Author Contributions: J.Z. conceived of, designed and performed the experiments. D.W. and P.Y. analyzed the data and discussed the results. W.L. participated in writing this paper.

Conflicts of Interest: The authors declare no conflict of interest.

References

1. Yi, H.; Xu, G.P.; Cheng, H.G.; Wang, J.S.; Wan, Y.F.; Chen, H. An overview of utilization of steel slag. *Proc. Environ. Sci.* **2012**, *16*, 791–801. [CrossRef]
2. Zhang, T.S.; Yu, Q.J.; Wei, J.X.; Li, J.X.; Zhang, P.P. Preparation of high performance blended cements and reclamation of iron concentrate from basic oxygen furnace steel slag. *Resour. Conserv. Recy.* **2011**, *56*, 48–55. [CrossRef]
3. Zhao, L.H.; Li, Y.; Zhou, Y.Y.; Cang, D.Q. Preparation of novel ceramics with high CaO content from steel slag. *Mater. Des.* **2014**, *64*, 608–613. [CrossRef]
4. Li, Z.B.; Zhao, S.Y.; Zhao, X.G.; He, T.S. Cementitious property modification of basic oxygen furnace steel slag. *Constr. Build. Mater.* **2013**, *48*, 575–579. [CrossRef]
5. Brand, A.S.; Roesler, J.R. Steel furnace slag aggregate expansion and hardened concrete properties. *Cem. Concr. Comp.* **2015**, *60*, 1–9. [CrossRef]
6. Shi, C.J. Characteristics and cementitious properties of ladle slag fines from steel production. *Cem. Concr. Res.* **2002**, *32*, 459–462. [CrossRef]
7. Shi, C.J. Steel slag- its production, processing, characteristics, and cementitious properties. *J. Mater. Civ. Eng.* **2004**, *16*, 230–236. [CrossRef]
8. Zhao, J.H.; Wang, D.M.; Wang, X.G.; Liao, S.C. Characteristics and mechanism of modified triethanolamine as cement grinding aids. *J. Wuhan Univ. Technol.* **2015**, *30*, 134–141. [CrossRef]
9. Yan, P.Y.; Mi, G.D.; Wang, Q. A comparison of early hydration properties of cement-steel slag binder and cement-limestone powder binder. *J. Therm. Anal. Calorim.* **2014**, *115*, 193–200. [CrossRef]
10. Kourounis, S.; Tsivilis, S.; Tsakiridis, P.E.; Papadimitriou, G.D.; Tsibouki, Z. Properties and hydration of blended cements with steel making slag. *Cem. Concr. Res.* **2007**, *37*, 815–822. [CrossRef]
11. Shi, Y.; Chen, H.Y.; Wang, J.; Feng, Q.M. Preliminary investigation on the pozzolanic activity of superfine steel slag. *Constr. Build. Mater.* **2015**, *82*, 227–234. [CrossRef]
12. Zhao, J.H.; Wang, D.M.; Yan, P.Y.; Zhao, S.J.; Zhang, D.W. Particle characteristics and hydration activity of ground granulated blast furnace slag powder containing industrial crude glycerol-based grinding aids. *Constr. Build. Mater.* **2016**, *104*, 134–141. [CrossRef]
13. Zhu, X.; Hou, H.B.; Huang, X.Q.; Zhou, M.; Wang, W.X. Enhance hydration properties of steel slag using grinding aids by mechanochemical effect. *Constr. Build. Mater.* **2012**, *29*, 476–481. [CrossRef]

14. Zhao, J.H.; Wang, D.M.; Liao, S.C. Effect of mechanical grinding on physical and chemical characteristics of circulating fluidized bed fly ash from coal gangue power plant. *Constr. Build. Mater.* **2015**, *101*, 851–860. [CrossRef]
15. Ghiasvand, E.; Ramezanianpour, A.A.; Ramezanianpour, A.M. Effect of grinding method and particle size distribution on the properties of Portland-pozzolan cement. *Constr. Build. Mater.* **2014**, *53*, 547–554. [CrossRef]
16. Han, C.J.; Yang, X.J.; Zhou, H.Q.; Tang, Y. Steel slag and its application in cement industries. *Mater. Rev.* **2010**, *24*, 440–443. (In Chinese)
17. Ghouleh, Z.; Guthrie, R.I.L.; Shao, Y.X. High-strength KOBM steel slag binder activated by carbonation. *Constr. Build. Mater.* **2015**, *99*, 175–183. [CrossRef]
18. Zong, Y.B.; Cang, D.Q.; Zhen, Y.P.; Li, Y.; Bai, H. Component modification of steel slag in air quenching process to improve grindability. *Tran. Nonferr. Met. Soc.* **2009**, *19*, s834–s839. [CrossRef]
19. Hou, G.H.; Li, W.F.; Wang, J.G. Difference of grindability and cementitious performance among minerals in steel slag. *J. Chin. Ceram. Soc.* **2009**, *37*, 1613–1617. (In Chinese)
20. Kong, L.Z.; Wang, J.; Chen, L.Z. Research on mineral phase and grindability of steel slag by changing components contents. *China Metall.* **2013**, *23*, 56–59. (In Chinese)
21. Zhou, Y.; Liu, H.B.; Dong, Y.C.; Chen, G.Y.; Liu, Y.L.; Wang, C. Research on grindability of steel slag by modifying. *China Metall.* **2010**, *20*, 38–41. (In Chinese)
22. Zhao, F.C.; Ju, J.T.; Liao, J.L.; Kong, W.M.; Dang, Y.J. Analysis of comprehensive utilization and basic properties of converter slag processed. *J. Iron Steel Res.* **2013**, *25*, 23–28. (In Chinese)
23. Choi, H.; Lee, W.; Kim, S. Effect of grinding aids on the kinetics of fine grinding energy consumed of calcite powders by a stirred ball mill. *Adv. Powder Technol.* **2009**, *20*, 350–354. [CrossRef]
24. Choi, H.; Lee, W.; Kim, D.U.; Kumar, S.; Kim, S.S.; Chung, H.S.; Kim, J.H.; Ahn, Y.C. Effect of grinding aid on the grinding energy consumed during grinding of calcite in a stirred ball mill. *Miner. Eng.* **2010**, *23*, 54–57. [CrossRef]
25. Gao, X.J.; Yang, Y.Z.; Deng, H.W. Utilization of beet molasses as a grinding aid in blended cements. *Constr. Build. Mater.* **2011**, *25*, 3782–3789. [CrossRef]
26. Toraman, O.Y. Effect of chemical additive on stirred bead milling of calcite powder. *Powder Technol.* **2012**, *221*, 189–191. [CrossRef]
27. Kim, H.S.; Kim, K.S.; Jung, S.S.; Hwang, J.I.; Choi, J.S.; Sohn, I. Valorization of electric arc furnace primary steelmaking slags for cement applications. *Waste Manage.* **2015**, *41*, 85–93. [CrossRef] [PubMed]
28. Sadique, M.; Al-Nageim, H.; Atherton, W.; Seton, L.; Dempster, N. Mechano-chemical activation of high-Ca fly ash by cement free blending and gypsum aided grinding. *Constr. Build. Mater.* **2013**, *43*, 480–489. [CrossRef]
29. Assaad, J.J.; Issa, C.A. Effect of clinker grinding aids on flow of cement-based materials. *Cem. Concr. Res.* **2014**, *63*, 1–11. [CrossRef]
30. Katsioti, M.; Tsakiridis, P.E.; Giannatos, P.; Tsibouki, Z.; Marinos, J. Characterization of various cement grinding aids and their impact on grindability and cement performance. *Constr. Build. Mater.* **2009**, *23*, 1954–1959. [CrossRef]
31. Altun, O.; Benzer, H.; Toprak, A.; Enderle, U. Utlization of grinding aids in dry horizontal stirred milling. *Powder Technol.* **2015**, *286*, 610–615. [CrossRef]

© 2016 by the authors; licensee MDPI, Basel, Switzerland. This article is an open access article distributed under the terms and conditions of the Creative Commons Attribution (CC-BY) license (http://creativecommons.org/licenses/by/4.0/).